a plurality of conducting segments, each segment being insulated from the others and

substrate for supporting the conducting segments, the substrate having a hole surrounded by the conducting segments and through which the primary particle beam passes; and

wherein a voltage is applied to at least two of the segments to deflect the particle beam traveling through the deflection units.

27. (Previously Presented) An objective lens system as recited in claim 22,

wherein the deflection unit includes twelve conducting segments arranged in four groups of three segments each; and

wherein a separate voltage is applied to each of the four groups of segments to deflect the primary particle beam.

28. (Currently Amended) An objective lens system as recited in claim [[23]] 27, wherein two of the four groups deflect the primary particle beam in the X direction and wherein the other two of the four groups deflect the primary beam in the Y direction.

29. (Currently Amended) An objective lens system as recited in claim [[24]] 28, wherein the X-direction and Y-direction groups are driven differentially.

REMARKS/ARGUMENTS

Claims 2, 4, 21, and 28-29 are amended by this response. Claims 3 and 5 are canceled. Accordingly, claims 2, 4, and 6-29 remain pending.

In the most recent office action, the Examiner requested that Applicants provide a copy of the following article: Chen et al., "The Optical Properties of 'Swinging Objective Lens' in a Combined Magnetic Lens and Deflection System with Superimposed Field"; Optik Vol. 64, pp. 341-347 (1983). A copy of this article is enclosed with this response.

The Examiner also requested copies of publications authored by the applicants, which describe swinging objective lens criteria. Accordingly, please also find enclosed with this response a copy of the following article: Chen et al, "Nanowriter: A new high-voltage electron

beam lithography system for nanometer-scale fabrication", Journal of Vacuum Science and Technology B, Vol.6 No.6, pp. 2009-2013 (Nov/Dec 1988).

Because the above reference copies are being provided at the request of the Examiner, they are not being submitted in the form of an information disclosure statement in order to avoid a certification and fee. The Examiner is therefore respectfully requested to formally cite these references in the next office action.

As an initial matter, Applicants appreciate the Examiner's indication of the allowable subject matter of claims 21-22 and 27-29. In accordance with the recommendation of the Examiner, claim 21 has now been amended to incorporate the elements of claim 2 prior to its amendment in the instant office action. Additionally, claim 28 is amended to now depend from claim 27 and thereby provide proper antecedent basis for the claim term "the four groups", and claim 29 is amended to depend from claim 28 and thereby provide proper antecedent basis for the claim term "the X-direction and Y-direction groups". Based upon these claim amendments, it is respectfully asserted that claims 21-22 and 27-29 are now in condition for allowance.

The Examiner had rejected a number of the pending claims as indefinite under 35 U.S.C. §112 ¶2. Claim 2 has now been amended to include the deflection unit element, thereby providing proper antecedent basis for this term in the dependent claims.

The Examiner also rejected a number of the pending claims as obvious under 35 U.S.C. §103, based upon the reference combination of U.S. patent no. 6,194,729 to Weimer et al. ("the Weimer patent") and U.S. patent no. 5,023,457 to Yonezawa ("the Yonezawa patent"), taken together or in combination with still other references. These claim rejections are overcome as follows.

As indicated in Figure 1 of the instant application (reproduced below), embodiments in accordance with the present invention relate to an objective lens system (112) for applying a particle beam (109) to a specimen (122):

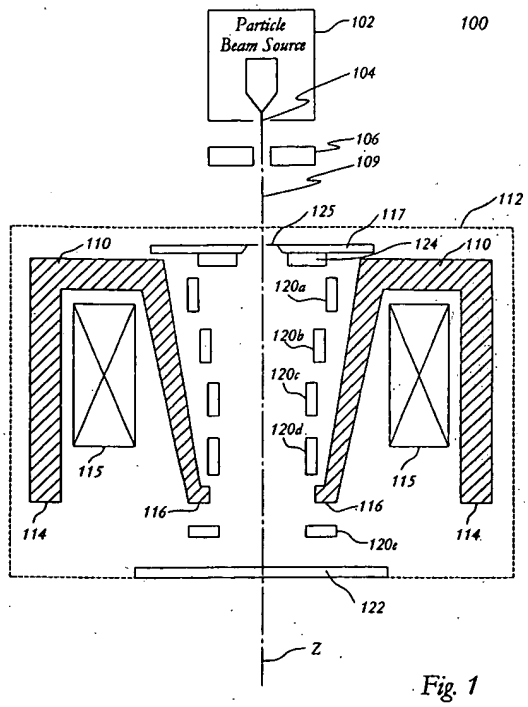

Fig. 1

a first set or "swinging group" of deflection units 120*a*, 120*d* and 120*e* is dedicated to the accurately but relatively slowly positioning of the focused beam over a precise point on the specimen within the deflection field of the lens . . . . A second set of deflection units 120*b* and 120*c* is dedicated to producing a more rapid scanning movement of the beam to cover an area . . . centered on the position determined by the first set of deflection units. (Emphasis added; page 8, lines 7-17)

As shown in Figure 1 above, at least one of the "swinging group" of deflecting units is located within the central bore of the lens. And as shown in Figure 5 of the instant application (reproduced in part below):

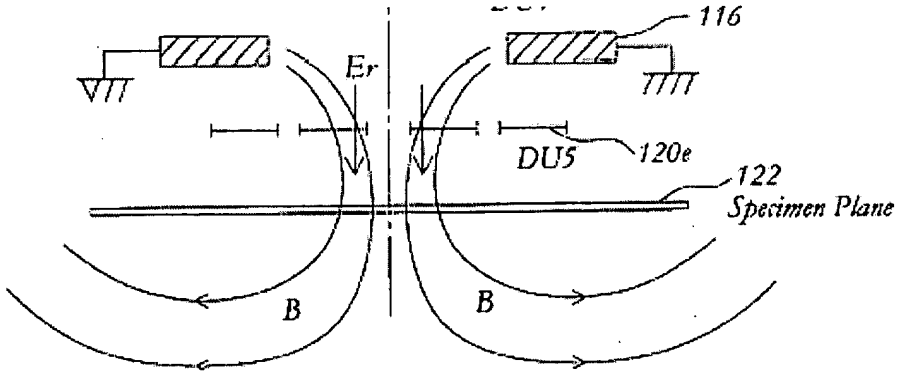

in certain embodiments at least one deflection unit (120*e*) lies in a retarding field (E*r*):

> Deflection unit 120*e* is particularly important to improving the size D in FIG. 4 of the deflection field over the specimen because it is closest to the specimen and in the retarding field produced by the specimen. Thus deflection unit 102*e* will have a large effect on the position of the particle beam because it is deflecting a beam with much lower energy than the deflection units 102*a*-102*d* and it is the deflection unit nearest the landing point of the beam on the specimen. (Emphasis added; page 8, lines 24-29).

Accordingly, pending independent claim 2 has been amended to recite:

> 2. An immersion lens system . . . comprising:
> . . . a deflection system including at least one deflection unit along a beam axis for deflecting the particle beam to allow scanning of the specimen, at least one deflection unit located in a retarding field of the beam, and at least one deflection unit located within the central bore of the lens . . . . (Emphasis added)

As a threshold matter, the Examiner is reminded that in order to establish a prima facie case of obviousness, "the prior art reference (or references when combined) must teach or suggest all the claim limitations." MPEP 2142. Here, the Weimer patent taken in combination with the Yonezawa patent, fails to teach or suggest a deflection system comprising a deflection unit located in a retarding field of the beam.

Figure 1 of the Weimer patent is reproduced below.

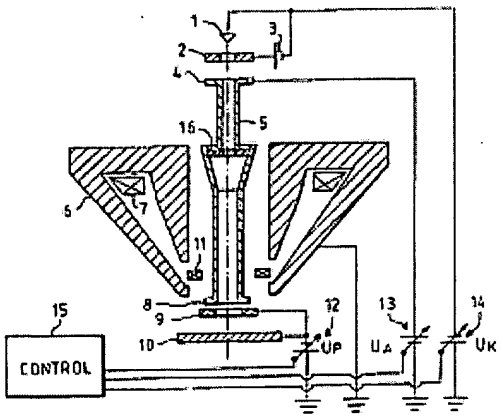

This, and all other Figures of the Weimer patent, show a deflection system comprising only a single unit (11) located within the within the pole piece (6) of the magnetic lens, outside any retarding field of the beam. (Col. 6, lines 30-35)

Similarly, Figure 1 of the Yonezawa patent is reproduced below.

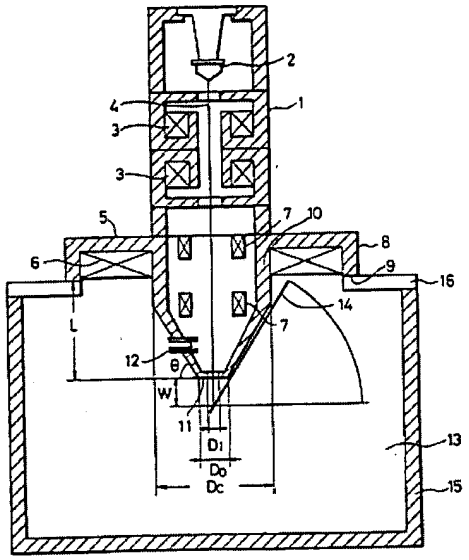

This and other Figures of the Yonezawa patent appear to depict a system comprising multiple beam deflection coils (7). Again, however, each such deflection coil is located within tube (10) and outside of any retarding field of the beam. (Col. 3, lines 42-43)

In the latest office action, the Examiner also rejected certain of the dependent claims as obvious based upon the Weimer and Yonezawa patent, in combination with U.S. patent no. 5,719,402 and U.S. patent no. 4,945,246. However, these references similarly fail to teach a deflection unit that is located within a retarding field of the beam.

Based at least upon the failure of the art relied upon by the Examiner, and in particular the Weimer and Yonezawa patents, to teach or even suggest a system having a deflection unit in the retarding field of the beam, it is respectfully asserted that the instant claims are not obvious. Accordingly, maintenance of these claim rejections by the Examiner is improper, and the claim rejections should be withdrawn.

In view of the foregoing, Applicants believe all claims now pending in this Application are in condition for allowance. The issuance of a formal Notice of Allowance at an early date is respectfully requested. If the Examiner believes a telephone conference would expedite prosecution of this application, please telephone the undersigned at 650-326-2400.

Respectfully submitted,

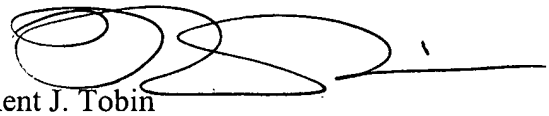

Kent J. Tobin
Reg. No. 39,496

TOWNSEND and TOWNSEND and CREW LLP
Two Embarcadero Center, Eighth Floor
San Francisco, California 94111-3834
Tel: 650-326-2400
Fax: 415-576-0300
KJT:ejt
60350077 v1

Optik 64, No. 4 (1983) 341–347 © Wissenschaftliche Verlagsgesellschaft mbH, Stuttgart

The optical properties of "Swinging Objective Lens" in a combined magnetic lens and deflection system with superimposed field

Zhong-wei Chen, Pei-yong Qiu, Jian-kun Wang

Shandong Engineering Institute
Jinan, China

Received 15 February 1983

Abstract

The concept of electro-magnetic swing of the focusing lens (Swinging Objective Lens) is proposed for improving the performance of electron beam scanning system. The third-order geometrical aberrations, in the Swinging Objective Lens, are greatly reduced. The distortion and the first order transverse chromatic aberration caused by the fluctuation in beam voltage are equal to zero, without considering the aberrations caused by predeflection coil. An arrangement based on "SOL" has been given to electron beam machine, which, with 5 cm working distance at the corner of 5 × 5 mm deflection field with 0.005-rad aperture and 1 in 10^4 beam voltage ripple, produces a total aberration disk of 0.083 μm before dynamic correction.

Inhalt

Die optischen Eigenschaften einer „schwingenden Objektivlinse" in einer Kombination aus magnetischer Linse und Ablenker mit überlagertem Feld. Zur Verbesserung von Ablenksystemen wird ein Objektiv mit schwingendem elektromagnetischen Feld (SOL) vorgeschlagen. Damit werden Aberrationen dritter Ordnung entscheidend gebessert. Verzeichnung und chromatische Queraberration durch Schwankungen der Strahlspannung werden zu Null, jedoch ohne Berücksichtigung der Aberrationen der Vorablenkung. SOL wurde in eine Elektronenapparatur eingebaut; hier hatte ein Ablenkfeld von 5 × 5 mm einen Arbeitsabstand von 5 cm, die Strahlapertur betrug 0,005 rad und die Schwankung der Strahlspannung 1:10^4; vor der dynamischen Korrektur ergab sich ein Bestrahlungsscheibchen von 0,083 μm.

Introduction

The electron beam exposure systems used in microfabrication have been rapidly developed since the 1970s. It is an important problem to eliminate or reduce deflective aberrations in a system for field scanning and precision lithography. A lot of work both in theory and in practice has been done about this subject [1]–[8].

The "Swinging Objective Lens" (SOL) proposed in present paper is a combined focusing lens and deflecting system, in which the optical axis of the objective lens is electro-magnetically swinged synchronously with the electron-beam deflected by pre-deflection coil in the first-order approximation. In this system, the third-order deflection distortion and the first-order transverse chromatic aberration caused by the fluctuation of voltage are equal to zero, and all third-order geometrical aberrations are greatly reduced without considering the aberrations caused by pre-deflection coil.

The third-order geometrical aberrations and the first-order chromatic aberrations in electron beam scanning system

The combined magnetic lens and deflection system consists of [2]:

a) A magnetic lens (or series of lenses) whose axis is the Z axis,
b) A pair (or series of pairs) of deflection coils,

whose axis of symmetry are the X and Y axis. The geometrical configuration of X and Y coil are assumed to be identical to one another.

The "object" of the combined system is assumed to be a point source placed on the Z-axis at the object plane Z_o. A real image of the point source is assumed to be focused at the image plane Z_i.

The paraxial trajectory equation of an electron is given by [2]:

$$W_1'' - iK\,[BW_1' + (1/2)\,B'W_1] = -iKDI \tag{1}$$

$$K = [e/(2m_0U)]^{1/2} \tag{2}$$

where i is the imaginary number unit, W_1 is a complex coordinate $W_1 = X + iY$, B is the axial flux density of the lens field, I is a complex current in the deflection coil $I = I_x + iI_y$, D is the axial flux density of deflection field with $I = 1\text{A}$, U is voltage of the electron beam, m_0 is mass of electron, e is charge of electron, and primes denote differentiation with respect to Z.

The corresponding homogeneous eq. (1) is the paraxial trajectory equation for the focusing system:

$$W_1'' - iK\,[BW_1' + (1/2)\,B'W_1] = 0 \tag{3}$$

Let the independent solutions of eq. (3) be $a(Z)$ and $b(Z)$ with following initial conditions

$$a(Z_o) = 0 \qquad a'(Z_o) = 1$$
$$b(Z_o) = 1 \qquad b'(Z_o) = 0 \tag{4}$$

For paraxial rays, the Helmholtz-Lagrange relation holds [2]:

$$a'b - ab' = \exp\,[2i\psi(Z)] \tag{5}$$

where $\psi(Z)$ is the rotation angle of electrons round the lens axis:

$$\psi'(Z) = (1/2)\, KB \tag{6}$$

Thus the solution of eq. (1) may be expressed as follows

$$W_1(Z) = a(Z)S_o + C(Z)I \tag{7}$$

where

$$C(Z) = -iKa(Z)\int_{Z_o}^{Z_i} D(\zeta)\,\bar{b}(\zeta)\,d\zeta + iKb(Z)\int_{Z_o}^{Z_i} D(\zeta)\,\bar{a}(\zeta)\,d\zeta \tag{8}$$

S_o is the slop of an electron trajectory at the object and $C(Z)$ is the trajectory for a unit deflection current.

The total third-order geometrical aberration ΔW_i is expressed in terms of S_i and W_i, where let S_i denote the half aperture tangent at the image plane i.e. $S_i = S_o a'(Z_i)$, and let W_i denote the image displacement caused by the deflection current i.e. $W_i = IC(Z_i)$. Thus

$$\begin{aligned}
\Delta W_i = {} & K_S S_i^2 \bar{S}_i && \text{(spherical aberration)}\\
& + K_L S_i \bar{S}_i W_i && \text{(coma length)}\\
& + K_R S_i^2 \bar{W}_i && \text{(coma radius)}\\
& + K_F S_i W_i \bar{W}_i && \text{(field curvature)}\\
& + K_A \bar{S}_i W_i^2 && \text{(astigmatism)}\\
& + K_D W_i^2 \bar{W}_i && \text{(distortion)}
\end{aligned} \tag{9}$$

Similarly the total first-order chromatic aberration ΔW_{1i} at the image plane Z_i is given by

$$\begin{aligned}
= {} & K_{TV} W_i \frac{\Delta V}{V} && \text{(transverse chromatic aberration caused by the fluctuation in beam voltage)}\\
& + K_{Te} W_i \frac{\Delta NI}{NI} && \text{(transverse chromatic aberration caused by the fluctuation in lens excitation)}\\
& + K_{TX} S_i \left(\frac{\Delta V}{V} - 2\frac{\Delta NI}{NI}\right) && \text{(axial chromatic aberration)}
\end{aligned} \tag{10}$$

The "Swinging Objective Lens" (SOL)

It is well known that in a prelens single deflection system, the deflective aberrations are greater than any other deflection systems. These aberrations are mainly caused by the electrons passing through the magnetic objective

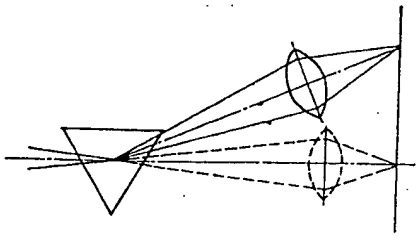

Fig. 1. The optical schematic diagram of "SOL" system.

lens. Under the focusing action of the magnetic lens the electrons rotate round the trajectory of the electron beam to focus the beam, at the same time the electron beam rotates round the axis of the lens. The first differentiation of rotation angle $\psi(Z)$ is expressed as:

$$\psi'(Z) = (1/2)\, KB \tag{11}$$

The rotation of the trajectory round the lens axis will add the focus of the beam. In the other hand, because of the rotation of the trajectory the electron beam will contract toward the lens axis. Thus when the electron beam arrives at the image plan the target will more approach the lens axis than without the influence of lens field. It means that the deflection quantity at the image plane will decrease and the electron beam will take a long way to reach the target. So the value of C' and C'' increase. Consequently, the value of those terms containing C' and C'' in the geometrical aberration coefficients increases. The effect of those terms can be seen from each geometrical aberration coefficient [2]. So that, in order to minimize the deflective aberrations, the control of the track of the deflecting principal trajectory becomes the key. Let the principal trajectory C pass through the lens linearly, as if the optical axis of the objective lens electro-magnetically swings synchronously to the deflected electron beam, and the deflection quantity at the image plane will increase, and the C', C'' decrease. In the first-order approximation this is a so-called swinging objective lens system. The optical schematic diagram of this "SOL" system is shown in fig. 1.

The paraxial trajectory equation of an electron in the combined magnetic lens and deflection system has already been given by eq. (1):

$$W_1'' - iK\,[BW_1' + (1/2)\, B'W_1] = -iKDI \tag{12}$$

Without considering the effect of pre-deflection, let D satisfy the following condition:

$$D = BC' + (1/2)\, B'C \tag{13}$$

Inserting eq. (13) in to eq. (12) and noticed that when $I = 1\,\mathrm{A}$, then $W_1 = C$, and we obtain following equation

$$C'' - iK\,[BC' + (1/2)\, B'C] = -iK\,[BC' + (1/2)\, B'C] \tag{14}$$

It is:

$$C'' = 0 \tag{15}$$

It means that the deflecting principal trajectory is a straight line. So it is seen that eq. (13) is the condition to realize Swinging Objective Lens. Without lossing generality, let

$$C = -\bar{C} \tag{16}$$

Inserting eq. (13)–(16) in to eq. (9) and (10), and making some simplifications, we obtain the following expressions for the third-order geometrical aberration coefficients and first- order chromatic aberration coefficients:

$$K_S = -\frac{1}{[\bar{a}'a'^2\bar{a}']_{z_i}} \int_{z_o}^{z_i} \{\bar{a}a'\bar{a}'a'' + (1/2)\,\bar{a}a'^2\bar{a}'' + iK\,[-(1/8)\,\bar{a}''a^2\bar{a}B' - (1/8)\,\bar{a}'a^2\bar{a}'B' + (1/8)\,\bar{a}a'^2\bar{a}B' + (1/8)\,\bar{a}aa''\bar{a}B']\}\,dz$$

$$K_L = -\frac{1}{[\bar{a}'ca'\bar{a}']_{z_i}} \int_{z_o}^{z_i} \{\bar{a}c'\bar{a}'a'' + \bar{a}a'c'\bar{a}'' + iK\,[(1/2)\,\bar{a}^2a'c'B' - (1/2)\,\bar{a}\bar{a}'ac'B']\}\,dz$$

$$K_R = \frac{1}{[\bar{a}'ca'^2]_{z_i}} \int_{z_o}^{z_i} \{-\bar{a}a'c'a'' + iK\,[(1/8)\,\bar{a}''a^2cB' - (1/4)\,\bar{a}a'^2cB' - (1/4)\,\bar{a}aa''cB' + (1/4)\,\bar{a}aa'c'B']\}\,dz$$

$$K_A = -\frac{1}{[\bar{a}'c^2\bar{a}']_{z_i}} \int_{z_o}^{z_i} \{(1/2)\,\bar{a}c'^2\bar{a}'' + iK\,[(3/8)\,\bar{a}^2c'^2B' + (1/8)\,\bar{a}''c^2\bar{a}B' + (1/8)\,\bar{a}'^2c^2B' - (1/2)\,\bar{a}\bar{a}'cc'B']\}\,dz$$

$$K_F = \frac{1}{[\bar{a}'a'c^2]_{z_i}} \int_{z_o}^{z_i} \{-\bar{a}c^2a'' + iK\,[(1/8)\,\bar{a}''ac^2B' - (1/2)\,\bar{a}a'c'cB' - (1/8)\,\bar{a}c^2a''B' + (1/2)\,\bar{a}ac'^2B']\}\,dz$$

$$K_D = 0$$

$$K_{TV} = 0$$

$$K_{Te} = -\frac{iK}{[\bar{a}'c]_{z_i}} \int_{z_o}^{z_i} \bar{a}\,[c'B + (1/2)\,cB']\,dz$$

$$K_{TX} = -\frac{iK}{[\bar{a}'a']_{z_i}} \int_{z_o}^{z_i} \bar{a}\,[-(1/2)\,a'B - (1/4)\,aB']\,dz$$

The application of "SOL"

Based on the concept of "SOL" a practical focus and deflection system used in electron beam exposure machine has already been made. It is well known that to be used in a real machine the structure must be easy to be manufactured and adjusted. In this deflection system two yokes are used as deflector, and every yoke is specially designed by computer so as to have the least deflection aberrations and easily to be made. One of the arrangements, with 5 cm working distance at the corner of 5 × 5 mm deflection field with 0.005-rad aperture and 1 in 10^4 beam voltage ripple, produces a total aberration disk (containing the influence of the first deflection yoke) of 0.083 μm before dynamic correction. Fig. 2 shows the distribution of the field on the axis.

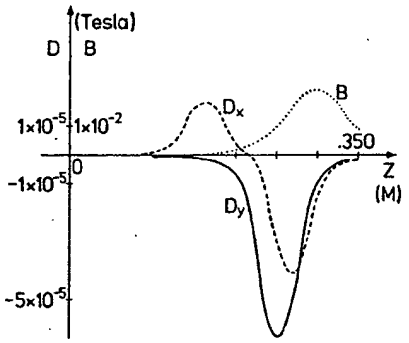

Fig. 2. The distribution of the magnetic deflection field *Dx*, *Dy* and objective lens field *B* on the axis for a practical electron beam machine.

Conclusions

In this paper the "Swinging Objective Lens" (SOL) for the combined magnetic lens and deflection systems with superimposed fields has been proposed in the first-order approximation. The condition to realize the SOL has been derived. The optical property of SOL has been given. From the aberration coefficients it can be seen that, excepting the effect of pre-deflec-

tion, the distortion and the transverse chromatic aberration caused by the fluctuation in beam voltage are equal to zero, the other aberrations (coma, astigmatism, field curvature) all reduced greatly. A practical use of SOL in electron beam machine has been given. It means that the SOL concept may be used in electron beam lithograph machine and other precision focusing and deflecting electron optical system.

Acknowledgements

The authors particularly wish to thank Prof. Ximen Jiye of Beijin University for his helpful discussion and critical reading of the manuscript.

References

[1] H. Ohiwa, E. Goto, A. Ono, Trans. Inst. Electron. Commun. Eng. Japan **54-B** (1971) 730.
[2] E. Munro, Optik **39** (1974) 450.
[3] E. Munro, J. Vac. Sci. Technol. **12** (1975) 1146.
[4] Ximen Jiye, Acta Physica Sinica **26** (1977) 34.
[5] E. Goto and T. Soma, Optik **48** (1977) 255.
[6] H. Ohiwa, Optik **53** (1979) 63.
[7] H. C. Pfeiffer, J. Vac. Sci. Technol. **12** (1975) 1170.
[8] H. C. Pfeiffer, G. O. Langner, J. Vac. Sci. Technol. **19** (1981) 1058.

Nanowriter: A new high-voltage electron beam lithography system for nanometer-scale fabrication

Z. W. Chen, G. A. C. Jones, and H. Ahmed
Microelectronics Research Laboratory, Department of Physics, Cambridge University, Cambridge Science Park, Cambridge CB4 4FW, England

(Received 1 June 1988; accepted 2 August 1988)

A new high-voltage electron beam lithography system, Nanowriter, has been designed and constructed to give a large scan field size without compromising the ability to write nanometer-scale structures. Nanowriter comprises a 100-kV LaB_6 electron gun with a zoom condenser arrangement consisting of two condenser lenses which are used to provide a system demagnification of up to 10 000 times. To combine a very small on-axis spot diameter of 4 nm and a large scanned field of $250 \times 250\ \mu m$ without dynamic correction, a newly developed swinging objective immersion lens (SOIL) concept based on variable axis immersion lens (VAIL) and swinging objective lens (SOL) has been utilized. The SOIL used here has four advantages: first, it is possible to reduce the working distance, thereby decreasing spherical aberration; second, the scanned field is increased without significantly increasing deflection aberrations; third, it permits easy alignment of the column, and fourth, an inherent attribute of the SOIL is the shielding from extraneous magnetic fields given to the target. The substrate resides on an in-lens stage which is supported on the boreless lower pole piece of the SOIL. The system has been used to delineate nanometer-scale patterns in poly(methylmethacrylate) (PMMA) resist. Lines of 15-nm width have been written into 50-nm-thick PMMA on thick Si substrates. These linewidths were almost unchanged over the whole scanned area of $250 \times 250\ \mu m$.

I. INTRODUCTION

Interest in the fabrication of structures with minimum dimensions in the nanometer-scale range has grown considerably over the last ten years. Much research has been carried out to explore the limits of microfabrication itself and many workers have utilized modified scanning electron microscopes (SEM's) or scanning transmission electron microscopes (STEM's). The fact that the resolution in these instruments is so high has made them the fundamental tools for basic nanostructure research[1–4] but in practice they offer only limited field size.

Nanowriter was built in response to the need to write patterns having ~10-nm features but with a much greater scanned field than that provided by modified SEM's or transmission electron microscopes which make it very difficult to use them to fabricate complex device structures without requiring a further stage of pattern delineation in other equipment. To increase the scanned field size, it is necessary to improve the electron optical performance of the column, especially the objective lens and deflection system. A newly developed SOIL (swinging objective immersion lens) based on variable axis immersion lens[5] (VAIL) and swinging objective lens[6] (SOL) has been designed for this purpose. The design of the SOIL, the performance of the optics, and some lithographic results obtained with this sytem are described below.

II. SYSTEM DESCRIPTION

The lithography system is shown schematically in Fig. 1. The electron optics uses design concepts drawn from both scanning electron microscopes and electron beam lithography systems. It consists of (i) a probe forming system to produce a focused beam of electrons, (ii) an electrostatic beam blanking unit, (iii) an octopole magnetic stigmator, (iv) the SOIL, optimized for a large scanned field and high resolution, (v) shallow junction backscattered electron detectors for focusing and registration purposes, (vi) a precision sample stage which slides on the lower pole piece of the objective lens and is driven by external micrometers, (vii) a

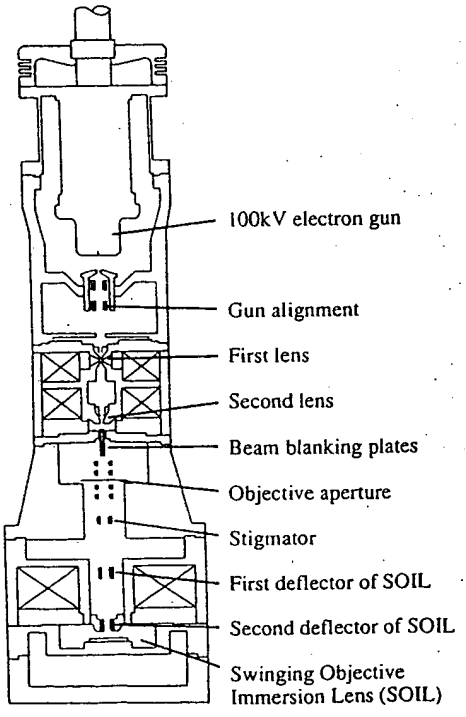

FIG. 1. Schematic cross section of the electron optical column.

pneumatically controlled floating air spring table, (viii) an electronic compensator for any residual extraneous magnetic fields, and (ix) a fast minicomputer interfaced to a vector scan pattern generator and the beam blanking unit.

The probe-forming system uses an LaB_6 electron gun which is capable of being operated over a voltage range 20–100 kV. The gun produces a crossover diameter of 20 μm with a brightness of 1×10^6 A cm^{-2} sr^{-1} at 25 kV. The condenser lens image position is kept constant while adjusting demagnification by using a two-lens zoom condenser, which is constructed so that the lenses are in precise axial alignment. These two lenses are followed by a swinging objective immersion lens to produce an overall demagnification from the source to target of $\times$ 10 000 together with a large scanning field of 250×250 μm, without dynamic correction.

Practical considerations, such as noise from the driving electronics, the ambient magnetic fields near the column, and the mechanical vibration of the table become increasingly important issues for large-area nanometer-scale writing, as are the normally negligible problems such as thermal noise and ground currents. Carefully chosen low-noise devices are used for the electronic circuits which are run at a low supply voltage. Optical isolators or differential receivers are used for all digital-to-analog interfacing and also for some of the long-distance analog signal paths in order to avoid ground loops. In addition to this, careful connection of each analog power supply ground is necessary.

Despite the inherent screening properties of the SOIL, some trouble was experienced with extraneous ac magnetic fields; in particular, frequency components at 50 and 150 Hz gave rise to a beam shift at the target of $\sim$25 nm peak to peak (p–p) at 50 kV accelerating potential. To reduce this problem, two sensor coils were installed at the most field-sensitive position of the column to sample the external fields in the X and Y directions. These signals were then amplified, phase shifted, and fed to the analog differential buffer of the deflection amplifiers in order to cancel the effect of these stray fields. The result was a fivefold reduction in the interference effects.

Vibration effects were reduced by using an air-spring isolation table with a natural frequency of 1 Hz to support the electron optical column, chamber, and vacuum diffusion pumps. The pumps contributed $\sim$9.5 nm of vibration at 1.3 kHz in the vertical plane above the pumps, due to the boiling of the oil. However, these vibrations were attenuated on reaching the optical column by a balanced bellows assembly and were found to be <0.5 nm in all planes in the region of the objective lens and chamber.

III. OBJECTIVE LENS AND DEFLECTOR SYSTEM

The objective lens and deflection system are the key parts of the optical system. The design goal was to focus a 4-nm diameter beam on a target with the scanned field as large as possible. In order to make it easy to adjust and operate the column, dynamic corrections to the beam are avoided. There are several types of magnetic scanning systems. In our system a modified double-deflection system with the second coil inside the lens is used. This structure is developed by the moving objective lens (MOL) concept.[7] The combined aberrations of focusing and deflection can be greatly reduced by using a second deflector placed inside the lens. This deflector moves the electrical center of the lens off axis but parallel, so that the deflected beam always passes through this new optical axis of the lens, hence it reduces the effect of the off-axis lens aberrations.

The swinging objective lens[6] enhances this principle. The electron, after deflection by the first pre-lens deflection coil, passes straight through the objective lens field to land on the image plane. To achieve this it is necessary to swing the ojective lens axis about a point, simultaneously with the beam as it is bent by the first deflector. The second deflector is used to swing the lens axis in synchronism. The SOL criterion defines the axial flux density distribution $B_{D2}(z)$ of the magnetic field of the second deflector. This is given in Eq. (1),

$$B_{D2}(z) = 0.5C(z)\cdot B'_{lens}(z) + C'(z)\cdot B_{lens}(z), \qquad (1)$$

where $B_{lens}(z)$ is the axial flux density of the lens field, $C(z)$ is the trajectory for a unit deflection current, and the prime denotes differentiation with respect to z.

The first term in $B_{D2}(z)$ is the magnetic field required for the MOL.[7] This field makes the axis of the lens move in a parallel manner away from the lens center. The second term in $B_{D2}(z)$ is required to swing the displaced lens axis towards the direction of the beam after being bent by the first deflection coil.

Using the "immersion" concept, the variable axis immersion lens[5] overcomes the problems associated with eddy current generation in the target area by removing one variable axis coil yoke and two compensating dynamic focus coils. This has been accomplished by replacing the lower pole piece of the variable axis lens (VAL) with a solid ferrite disk. Incorporating this immersion concept into SOL, we arrive at the SOIL system. This has both the advantages of the VAIL and the single-bore objective lens system[8] of eliminating the stray field problems by total magnetic shielding of the target and of simplifying the mechanical alignment of pole pieces. A more important advantage for SOIL is that, with the immersion lens, the SOL criterion can be correctly matched for use with a smaller working distance and large scanning field without resorting to dynamic corrections. Figure 2 shows the immersion lens axial field distribution $B_{D2}(z)$ and the magnetic field of the second deflector $B_{D2}(z)$ defined by SOL concept. It can be seen that this field is very similar to that produced by a toroidal coil.

Lens design programs were used to calculate, the magnetic field distribution on the axis of the objective lens.[9] A further computer program for calculating third-order geometrical aberrations and first-order chromatic aberrations, for a combined focusing and deflection system, has been developed by the authors. This program was used to calculate the optical properties of the SOIL system.

In an ideal SOIL, many aberrations caused by the objective lens field are compensated, but the aberrations caused by the first pre-lens deflection coil field are not compensated. An off-axis beam of electrons passing through a lens field is caused to rotate about the lens axis while the electrons themselves spin in the same sense around the beam axis. The application of a second magnetic field (by the second deflec-

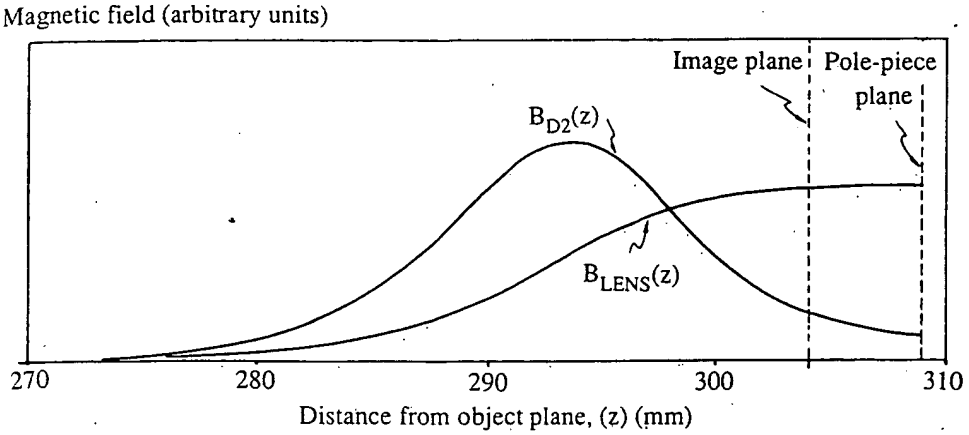

FIG. 2. The immersion lens field distribution $B_{lens}(z)$ and the magnetic field distribution of the second deflector $B_{D2}(z)$ defined by the swinging objective lens criterion.

tor) can be used to oppose this rotation and hence the spin. The net effect is twofold: first, the deflected beam is not brought back towards the lens axis by the focusing action of the lens, therefore the net deflection is increased; and second, the reduced spin of the beam results in an increase of the focal length of the lens which is the requirement to reduce field curvature aberration. To determine the best parameters an optimization program was developed which, after being given the lens and initial deflector parameters, systematically attempts to iterate to the best design of deflectors. This was carried out using a purpose written "Mass Complex" optimization method. This program attemps to find a deflector geometry that minimizes the sum of the squares of the aberrations, before dynamic correction, subject to specified constraints on the lens and deflector dimensions. The parameters which can be changed by the optimization program are (i) the geometry and axial locations of the two deflectors, (ii) the drive current ratio of the second to first deflector, (iii) the rotation angle between the first and the second deflector, and (iv) the geometrical form of the second deflector.

After running the optimization program, it is sometimes found that the chosen lens structure is not ideal and another design iteration is necessary following a slight modification of the lens structure. After the optimization, the trace of the beam trajectory from object point to image point is carefully checked as this trajectory will show whether or not the design is stable, whether the performance is critically dependent on small changes in the dimensions of the structure.

The deflected beam trajectory in the SOIL from object point to image point in an optimized SOIL system is shown schematically in Fig. 3. The electron in passing through the first deflector is bent by the magnetic field B_{D1}. The electron enters the immersion lens field, spins about the beam axis due to the force from the lens field, which causes the focusing of the beam. At the same time, the lens field forces the beam to rotate around the symmetry axis of the objective lens by force F_L. This rotation is countered by the force F_{D2}, which arises from the properly optimized second deflector field B_{D2}, so that the beam passes initially without rotation through the lens. Before the beam lands at the image plane, it is found that for an optimized system, the beam has to be slightly overcompensated so that a small rotation actually takes place in the opposite direction to that of the lens. In essence it means that this antifocusing rotation compensates further the curvature aberration caused by the first deflector. The calculated performance parameters of the SOIL used in our system are shown in Table I.

The SOIL system with a 15-mm gap between upper and lower pole pieces and a 20-mm diam hole in the upper pole piece is shown in Fig. 4. The SOIL has a spherical aberration coefficient of 4.3 mm and an axial chromatic aberration coefficient of 5.4 mm. The sample stage, made from aluminum and having overall dimensions of 35×25 mm, slides on the lower pole piece of the objective lens. A small Faraday cup is also mounted on the stage in order to measure the beam

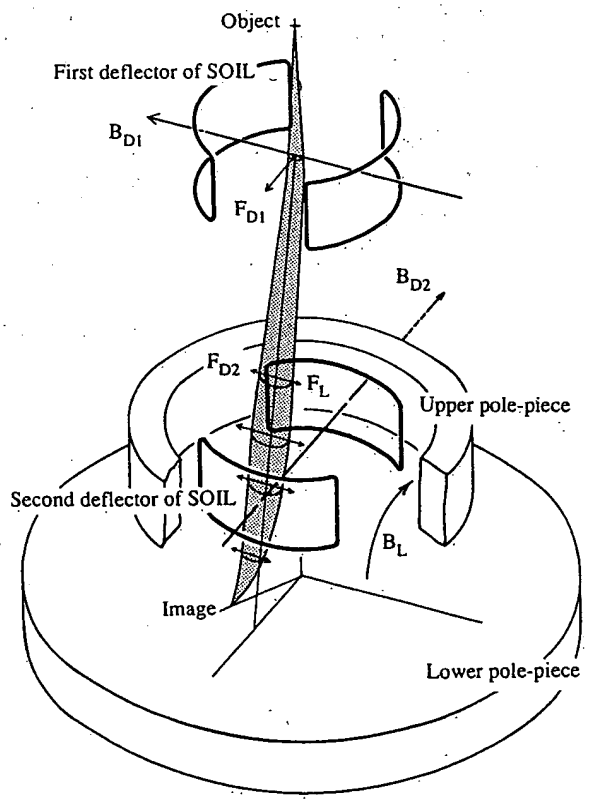

FIG. 3. The beam trajectory in the SOIL from object point to image point in an optimized system, where B_{D1} and B_{D2} are the magnetic fields of first and second deflection coils, respectively, F_{D1} and F_{D2} the forces on electrons from B_{D1} and B_{D2}, $B_{lens}(z)$ is the lens magnetic field distribution, and F_L is the force on electrons from B_{lens}.

TABLE I. Aberrations at corner of image plane.

Field size for deflection	250	μm
Beam voltage	100	kV
Aperture semiangle	4.0	mrad
Beam voltage ripple	2.5	V
	Axial	Overall
Distortion (isotropic)		0.05
Distortion (anisotropic)		2.2
Spherical aberration	0.14	0.14
Coma (isotropic)		0.081
Coma (anisotropic)		0.66
Field curvature		0.071
Astigmatism (isotropic)		0.75
Astigmatism (anisotropic)		1.1
Axial chromatic	-0.5	-0.5
Transverse chromatic (isotropic)		0.44
Transverse chromatic (aniso)		0.61
Overall aberration	0.56	1.9 nm

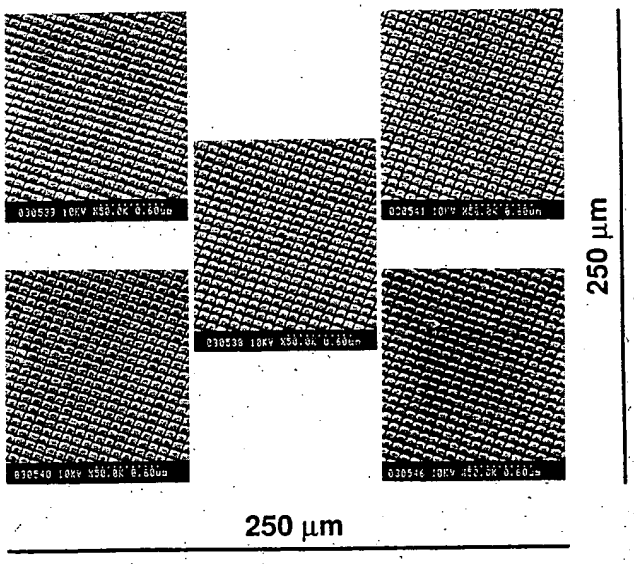

FIG. 5. Grid structures exposed in PMMA resist at the center and four corners of a 250×250 μm field (35° tilt in SEM).

current. Two samples of 5×5 mm may be mounted on this stage simultaneously which can then be mechanically traversed over a 15×13-mm field by external micrometer drives. The flatness of the stage is to within 2 μm over a 5-mm field. Shallow-junction silicon diodes located beneath the upper pole piece of the lens detect the backscattered electron signal for focusing and registration purposes.

IV. LITHOGRAPHIC PERFORMANCE

Poly(methylmethacrylate) (PMMA) resist films of 25 to 50 nm thickness were used together with hexamethyldisilazane (HMDS) adhesion promoter. After coating with the resist, a small area of 60-nm-thick gold–palladium was evaporated onto the edge of the sample and baked for 30 min at 175 °C; which produced cracks in the gold–palladium film. These cracks were used as a target for focusing using the backscattered electron detector.

The system performance was checked by measuring the resolution at the center and edges of the scan field. Grid structures of area 100×100 nm were written at the center

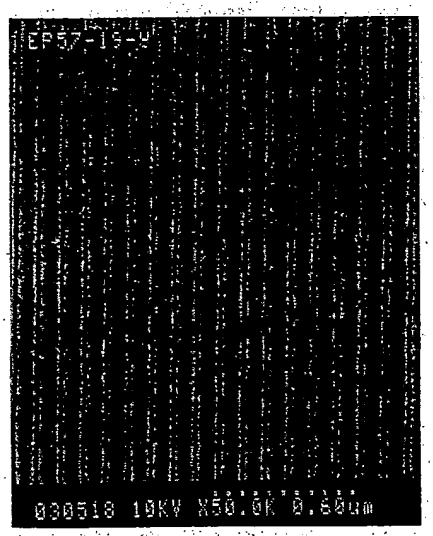

FIG. 6. Exposed PMMA resist structures showing 15-nm wide lines with 0.1-μm spacings.

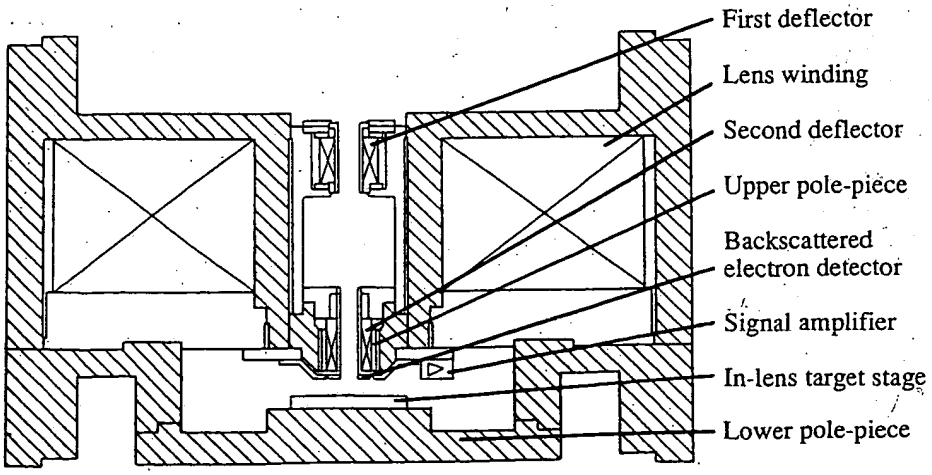

FIG. 4. Schematic cross section of the swinging objective immersion lens.

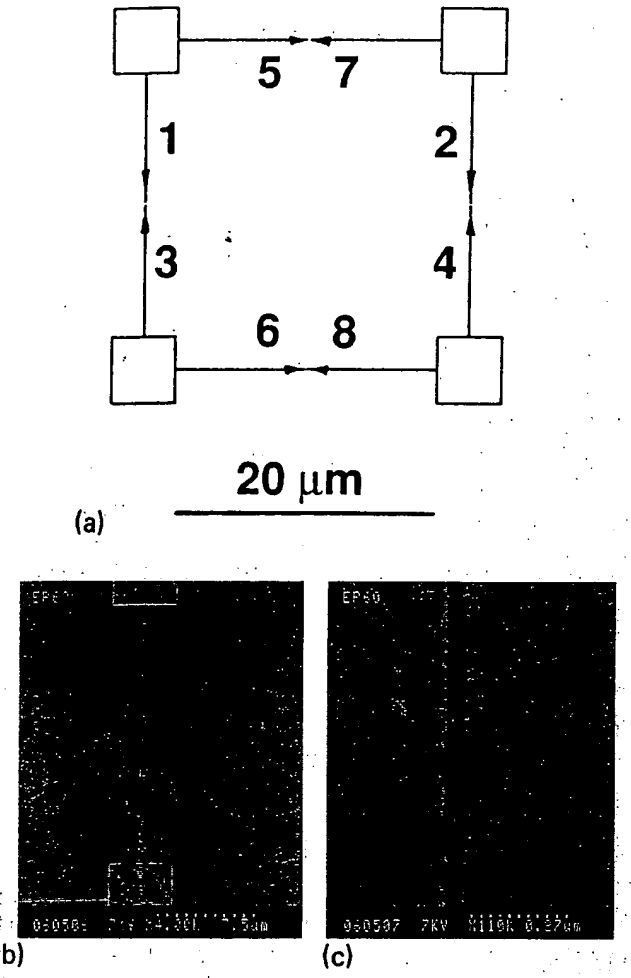

FIG. 7. The test demonstrates patterns the absence of any line misplacement due to deflection hysteresis: (a) exposure strategy, (b) exposed lines between pads, and (c) high-magnification micrograph of the join between the two lines.

and at the four corners of the 250×250-μm field. A beam current of 5×10^{-12} A and a line dose of 1.6 nC cm^{-1} at 60 kV was used. The samples were developed in a solution of 3:7 Cellasolve in methanol.[8] The 13-s development was followed by a 30-s rinse in pure methanol.

Figure 5 shows a set of SEM micrographs taken with a sample tilt angle of 35°. From these micrographs it can be seen that a linewidth of ~15 nm was obtained at all points within the 250×250-μm field, except in the bottom right-hand corner, where 20 nm was obtained. This may be due to a tilt of the sample on the stage or a misaligned deflection coil. Figure 6 shows 15-nm lines in PMMA.

The effect of hysteresis was checked and the results are shown in Fig. 7. First four 5×5 μm square pads were exposed, followed by eight individual lines (numbered 1–8) drawn consecutively, in the directions shown. Hysteresis in the deflection field would have caused the line between each pair of pads to be discontinuous. Figure 7(b) shows a pair of lines betweeen two of the pads. Figure 7(c) shows the joint in these two lines. No hysteresis effects can be seen. It may be concluded that the Nanowriter, with its swinging objective immersion lens, has enabled the lithography of structures below 20 nm over a large scanned field of 250×250 μm.

ACKNOWLEDGMENTS

The authors wish to acknowledge the technical contribution of the members of the Cavendish and the Microelectronics Research Laboratory workshops, in particular, S. Brown and N. Holmes. The help of S. Blythe and T. S. Norris is acknowledged. Financial support provided by Trinity College and Cavendish Laboratory, Cambridge University, is acknowledged.

[1] A. N. Broers, W. W. Molzen, J. J. Cuomo, and N. D. Wittels, Appl. Phys. Lett. **29**, 596 (1976).
[2] K. L. Lee and H. Ahmed, J. Vac. Sci. Technol. **19**, 946 (1981).
[3] R. E. Howard, H. G. Craighead, L. D. Jackel, and P. M. Mankiewich, J. Vac. Sci. Technol. B **1**, 1101 (1983).
[4] M. Isaacson and A. Murray, J. Vac. Sci. Technol. **19**, 1117 (1981).
[5] M. A. Sturans and H. C. Pfeiffer, *Microcircuit Engineering 83*, edited by H. Ahmed, J. R. A. Cleaver, and G. A. C. Jones (Academic, London, 1983), p. 107.
[6] Z. W. Chen, P. Y. Qiu, and J. K. Wang, Optik **64**, 341 (1983).
[7] H. Ohiwa, E. Goto, and A. Ono, Electron. Commun. Jpn. B **54** (1971).
[8] T. H. Newman, K. E. Williams, and R. F. W. Pease, J. Vac. Sci. Technol. B **5**, 88 (1987).
[9] E. Munro, Ph.D. thesis, Cambridge University, 1971.